

# Real time optical characterization of gas flow dynamics in high-pressure chemical vapor deposition

Vincent Woods,<sup>a)</sup> Harald Born, Martin Strassburg, and Nikolaus Dietz  
*Department of Physics and Astronomy, Georgia State University, Atlanta, Georgia 30030*

(Received 4 December 2004; accepted 23 February 2004; published 21 July 2004)

While low-pressure chemical vapor deposition (CVD) methods offer excellent pathways for many compound semiconductors, these growth techniques possess limitations in the growth of high quality compounds with large thermal decomposition pressure such as InN and related materials. To study and extend the growth towards elevated pressures a high-pressure CVD system with integrated real time optical characterization techniques has been established. The built-in real time monitoring techniques allow the characterization of gas flow kinetics, precursor decomposition kinetics, as well as the crucial steps of nucleation and film formation. In this contribution, we report the characterization of process parameter under which the thin film growth process can be maintained under laminar flow condition. Laser light scattering has been proven as the most robust optical tool to characterize the onset of turbulence. Hence, it allows the mapping the pressure and flowing regime under which laminar flow can be maintained. © 2004 American Vacuum Society. [DOI: 10.1116/1.1705589]

## I. INTRODUCTION

Solid solutions of group III nitrides, in particular of the GaN–InN system, are presently under intense development for optoelectronic and microelectronic applications. High quality Ga-rich epilayers of  $\text{Ga}_x\text{In}_{1-x}\text{N}$  can be fabricated successfully by traditional low-pressure chemical vapor deposition (CVD) methods that focus on low-pressure processes in order to minimize the influence of flow dynamics on growth conditions. However, low-pressure deposition processes are limited to a regime where the partial pressures of the constituents do not differ vastly and the decomposition process can be countered by off-equilibrium process conditions. In particular, the small formation enthalpy of InN hampers its epitaxial growth.<sup>1</sup> Off-equilibrium conditions such as employed in molecular beam epitaxy (MBE) and organometallic (OM) (CVD) growth of InN require low growth temperature to overcome the thermal decomposition pressures,<sup>2–5</sup> which limits the quality of InN and In rich  $\text{Ga}_x\text{In}_{1-x}\text{N}$  epilayers. Due to the low temperatures, extremely high V–III ratios have to be applied to prevent the formation of metal droplets on the surface.<sup>5–7</sup> Meanwhile, theoretical considerations suggest the employment of smaller V–III ratios.<sup>8</sup> Therefore, approaches to InN growth must be explored. A CVD growth technique utilizing elevated pressure is required in order to stabilize the surface of InN at optimal processing temperatures. A high background pressure of nitrogen has been shown to stabilize the surface of InN at elevated temperatures<sup>9</sup> but has not yet been incorporated into a CVD growth scheme. Therefore, growth of InN at higher pressures (1–100 bar) is expected to expand the processing window towards higher temperatures, leading to an improved crystalline quality and providing a closer match to the optimal processing temperature of InN.

However, the growth in an elevated pressure regime re-

quires an assessment of the thermodynamic driving force and kinetic limitations of growth for understanding and optimization of high-pressure organometallic chemical vapor deposition (HPOMCVD) processes. The maintenance of laminar flow conditions during CVD growth is also crucial in order to provide homogeneous growth conditions.

In order to gain insights in the growth dynamics of HPOMCVD, we constructed a high-pressure reactor system for the growth of group III nitrides that incorporates real time optical characterization capabilities. Only optical diagnostics will provide the real time information pertaining to gas flow dynamics in the reactor, allowing the characterization of laminar and turbulent flow regimes. In the following we introduce the high-pressure reactor design and the real time optical techniques used to characterize the gas flow conditions in the flow channel reactor. The characterization of the gas flow conditions in the reactor system are presented and analyzed in order to determine the process parameter under which laminar and turbulent flow can be maintained.

## II. HIGH-PRESSURE REACTOR

The growth of group III nitrides under high-pressure CVD conditions utilizing real time optical characterization requires the use of a reactor system design. A detailed description of our HPOMCVD reactor is presented in previous publications.<sup>10–12</sup> Figure 1 schematically illustrates the high-pressure reactor system which is composed of: (a) a flow channel CVD reactor, (b) a control and data acquisition system, and (c) a gas flow and pressure control system with pulsed precursor compression and injection.

The high-pressure CVD (HPCVD) reactor can be operated from atmospheric pressure up to 100 bar. The reactor provides optical access ports for the real time monitoring of gas flow dynamics and precursor decomposition kinetics. Additional optical access ports allow the monitoring of the growth surface itself. Constant pressure and flow conditions

<sup>a)</sup>Electronic mail: vwoods1@student.gsu.edu

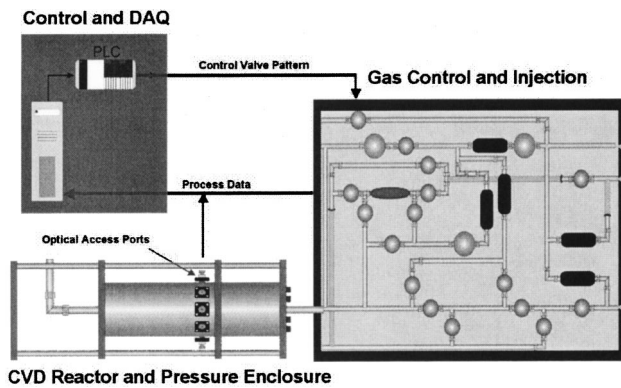


FIG. 1. Schematic illustration of high-pressure OMCVD system including the reactor and pressure enclosure, control and data acquisition and gas control and injection system.

in the reactor are maintained by the gas control and injection system. In addition, the gas control system provides for the compression of chemical precursors, (via carrier gas) and the subsequent timely controlled injection in the reactor. The temporally separated injection of precursors is important in order to suppress gas phase reactions, which become dominant in a dense gas phase. The system is fully computer controlled and utilizes a programmable logic controller to provide precise synchronization between precursor injection and optical data acquisition.

Figures 2(a) and 2(b) depict the reactor flow channel assembly in the HPOMCVD reactor. Figure 2(a) shows one half of the reactor flow channel, which is symmetric in design. According to the applied design consistent thermal conditions are provided and simultaneous optical measurements from two substrates are enabled. The symmetry substrate/heating design provides an uniform heat profile in the reactor channel and avoids an undesired deposition on the opposite reactor channel. To maintain laminar flow conditions, the cross-sectional area is kept constant through out the flow channel. Figure 2(b) depicts the cross-sectional view of the center section of the reactor flow channel. The flow channel can be seen along the center axis of the assembly. The reactor flow channel in the center section is 50 mm in width and 1 mm in height.

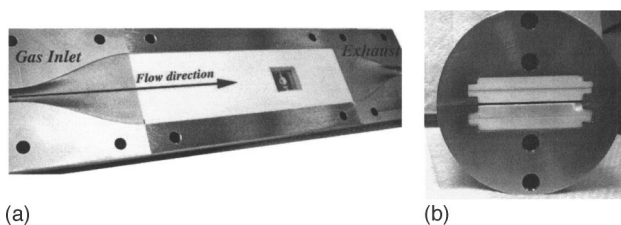


FIG. 2. (a) Half of the reactor flow channel assembly showing flow direction. The flow channel is designed with a constant cross-sectional area for the maintenance of laminar flow. The sapphire substrate is seen along center axis of flow and is held in two  $\alpha$ - $\text{Al}_2\text{O}_3$  plates. (b) Cross-sectional view of the center section of the reactor flow channel assembly. The flow channel is visible along the center axis of the assembly between the sets of  $\alpha$ - $\text{Al}_2\text{O}_3$  plates.

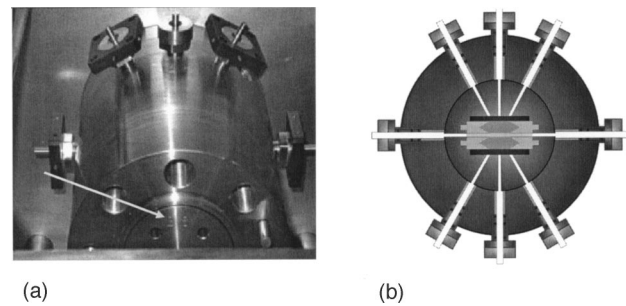


FIG. 3. (a) Cross-sectional view of the open pressure enclosure. The top half of reactor flow channel assembly is indicated by the arrow. The two optical access ports to flow channel are shown on the sides and three of the six access ports to substrate are shown on the top. (b) Schematic illustration showing the cross-section view of the reactor system. The two optical access ports to the flow channel are illustrated on the sides.

The reactor flow channel assembly is contained in a high-pressure enclosure, which can sustain pressures up to 100 bar. Figure 3(a) provides a view at the open high-pressure enclosure with the inserted flow channel reactor (arrow). The optical access ports are visible on both the top and sides of the pressure enclosure. These optical access ports enable the optical monitoring perpendicular to the flow direction along the centerline of the substrate as shown schematically in Fig. 3(b). Two ports provide access to the flow channel and allow characterization of the gas flow conditions and gas phase reactions. Each half of the symmetric reactor provides three optical access ports to the backside of the substrate for the characterization of surface chemistry, thin film nucleation, and coalescence, and for scattering processes from the gas phase.

### III. CHARACTERIZATION OF FLOW DYNAMICS AND LAMINAR FLOW REGIME

Maintaining laminar flow is crucial in CVD reactor systems in order to provide a consistent supply of precursor constituents that allows the correlation of gas phase constituent concentrations to the diffusion process and to the surface chemistry processes which drive the thin film growth. Therefore, the first task is to establish the process conditions under which laminar flow can be maintained. To characterize the

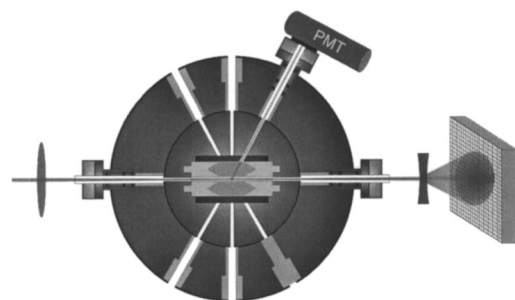


FIG. 4. Cross-sectional view of the HPOMCVD reactor showing optical access ports utilized for real time characterization of gas flow conditions. Laser light is focused to the center of the flow channel. Laser beam profile analysis was performed using a CCD camera. The forward component of the laser light scattering intensity was measured with a photomultiplier tube.

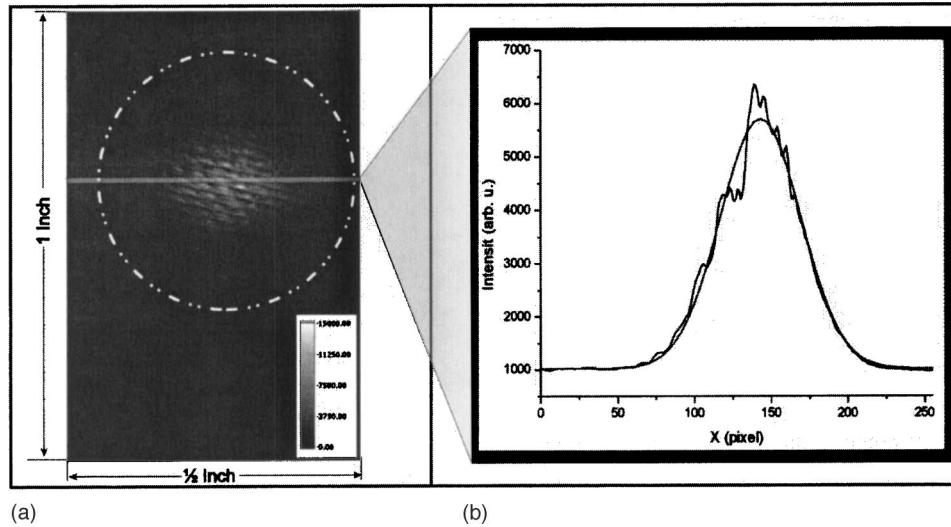


FIG. 5. (a) CCD image of the laser beam at normal incidence. The variations in intensity are due to imperfections in the optical access ports. The dotted circle indicates the radius of the access port and the light band indicates the location of the profile analysis. (b) Profile analysis of the CCD image of the laser beam at normal incidence showing CCD intensity as a function of location and Gaussian fit. The variations in intensity due to optical access port imperfections are clearly visible.

gas flow dynamics, two real time optical characterization techniques were utilized simultaneously; laser beam profile analysis and laser light scattering (LLS). As schematically illustrated in Fig. 4, laser light was focus through an optical access port at the center of the flow channel. The transmitted beam passes through an exit rod, where the beam size is expanded and the intensity distribution analyzed via a charge coupled device (CCD) array. Simultaneously, a photomultiplier tube was employed to monitor the forward component of LLS. The flow rates were varied from 3 to 21 slm for a given constant reactor pressure. The optical monitoring experiments were performed for both increasing and decreasing flows.

For laminar flow conditions, an uniform gas density is expected that results in a homogeneous index of refraction throughout the reactor flow channel. As the flow moves in a

turbulent flow regime, density fluctuations are introduced in the flow channel. The resulting temporal and spatial variation in the index of refraction is expected to increase the LLS intensity and to broaden the Gaussian laser beam profile. Images of the laser beam intensity were monitored by the CCD array at varied flows and pressures. A representative image is shown in Fig. 5(a) with the outline of the optical access port indicated by a dotted circle. The intensity variations of the laser beam image are due to imperfections in the fused silica rods uses as optical access ports. Beam profile analysis has been performed in order to fit a Gaussian distribution to the beam profile and is shown in Fig. 5(b). The imperfections in the fused silica rods introduced an additional broadening in the laser beam profile, which is superimposed to the beam broadening expected for turbulent flow conditions. The error bars obtained from the analysis for dif-

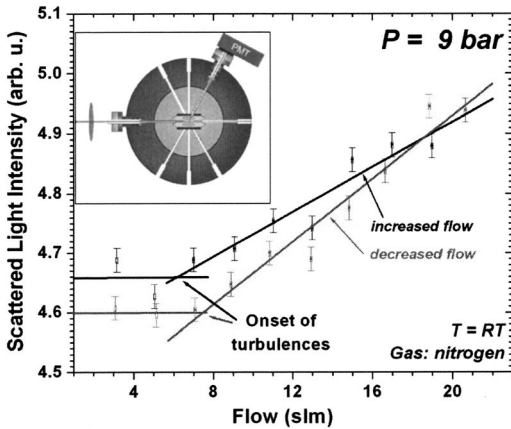


FIG. 6. Scattered light intensity as a function of gas flow. These data were collected at 9 bar for flows of 3–21 slm. The onset of the increase in intensity corresponds to the transition from laminar to turbulent flow and occurs at approximately 7 slm.

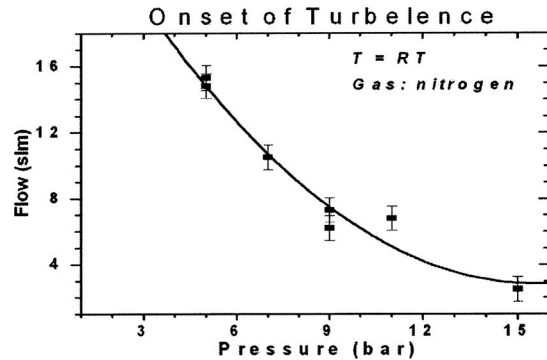


FIG. 7. Summary analysis of the transition from laminar to turbulent flow conditions as determined by LLS intensity measurements. Data reveal that the onset of turbulence occurs at decreased flow rates for increased pressures. The line connecting the onset points serves as a guide to the eye below which pressure and flow rate settings are expected to result in laminar flow conditions.

ferent flows and pressures indicated the laser beam profile analysis is not a reliable flow characterization technique.

The analysis of the simultaneous monitored LLS intensity showed surprisingly good results, which allowed focusing solely on LLS analysis for the characterization of the flow dynamics. The LLS intensities as a function of flow rate at a constant pressure are depicted in Fig. 6. The data were collected under constant pressure (9 bar) conditions and flow rates between 3 and 21 slm. The LLS intensity remains constant for flow rates below a critical point of approximately 7 slm. For flow rates above the critical point, a monotone increase in the intensity of LLS is observed. The region (“*transition point*”) where the steady LLS intensity begins to increase indicates a transition from a laminar to turbulent flow condition. In order to determine the laminar/turbulent *transition point* for our HPOMCVD reactor, the LLS intensities were measured and analyzed for pressures between 5 and 15 bar and flow rates from 3 to 21 slm.

The LLS analysis is summarized in Fig. 7 which shows the onset of turbulent flow (*transition point*) as a function of pressure and flow rate. As indicated, the onset of turbulent flow occurs at lower flow rates for increased pressures. This behavior is expected from the definition of the Reynolds number,  $Re = \rho ul / \eta$ , where  $\rho$  is the density and  $\eta$  is the viscosity of the gas,  $l$  is a characteristic length determined by the geometry of the flow channel, and  $u$  is the flow velocity. Moreover, the density is proportional to the pressure of the gas. The obtained results support the inverse relationship between flow rate and pressure in laminar/turbulent flow transitions. The LLS analysis indicates that for the high-pressure flow channel reactor laminar process condition can be maintained for flows up to 20 slm and pressures up to 20 bar.

#### IV. CONCLUSIONS

We analyzed the flow dynamics in a high-pressure flow channel reactor utilizing its integrated real time optical char-

acterization capabilities. The process window for laminar growth conditions has been established by analyzing the LLS intensity as a function of flow rate and pressure. The analysis determined the onset of turbulent flow as the transition point where the LLS intensity monotone increases. Laminar flow conditions can be maintained in a processing window of pressure ranges from 1 to 15 bar and flow rates from 3 to 21 slm. LLS has been demonstrated as a simple and robust tool for the characterization of gas flow conditions.

#### ACKNOWLEDGMENTS

This work has been supported by NASA under Grant No. NAG8-1686. M.S. gratefully acknowledges the support of the Alexander von Humboldt-Foundation.

<sup>1</sup>D’Ans Lax, in *Taschenbuch für Chemiker und Physiker, Band I*, edited by E. Lax and C. Synowietz (Springer, Berlin, 1967).

<sup>2</sup>C. R. Abernathy, S. J. Pearton, F. Ren, and P. W. Wisk, *J. Vac. Sci. Technol. B* **11**, 179 (1993).

<sup>3</sup>W.-K. Chen, Y.-C. Pan, H.-C. Lin, J. Ou, W.-H. Chen, and M.-C. Lee, *Jpn. J. Appl. Phys., Part 2* **36**, L1625 (1997).

<sup>4</sup>S. Yamaguchi, M. Kariya, S. Nitta, T. Takeuchi, C. Wetzel, H. Amano, and I. Akasaki, *J. Appl. Phys.* **85**, 7682 (1999).

<sup>5</sup>T. Schmidting, M. Drago, U. W. Pohl, and W. Richter, *J. Cryst. Growth* **248**, 523 (2003).

<sup>6</sup>O. Ambacher *et al.*, *J. Vac. Sci. Technol. B* **14**, 3532 (1996).

<sup>7</sup>T. Matsuoka, H. Okamoto, M. Nakao, H. Harima, and E. Kurimoto, *Appl. Phys. Lett.* **81**, 1246 (2002).

<sup>8</sup>For example, U. Großner, J. Furthmüller, and F. Bechstedt, *Appl. Phys. Lett.* **74**, 3851 (1999).

<sup>9</sup>J. B. McChesney, P. M. Bridenbaugh, and P. B. O’Connor, *Mater. Res. Bull.* **5**, 783 (1970).

<sup>10</sup>N. Dietz, S. McCall, and K. J. Bachmann, Proceedings of the Microgravity Conference 2000, Huntsville, AL, 6–8 June 2000, NASA/CP-2001-210827, 2001, pp. 176–181.

<sup>11</sup>S. D. McCall and K. J. Bachmann, *Mater. Res. Soc. Symp. Proc.* **693**, I3.13.1 (2002).

<sup>12</sup>N. Dietz, V. Woods, S. McCall, and K. J. Bachmann, Proceedings of the Microgravity Conference 2002, Huntsville, AL, 25–26 June 2002, NASA/CP-2003-212339, 2003, pp. 169–181.